

Full Length Research Paper

Digital orange tree: An intelligent agent based simulation model

Hongchun Qu^{1*}, David Norman² and Zhonghua Lu³

¹Key Laboratory of Network Control and Intelligent Instrument (Chongqing University of Posts and Telecommunications), Ministry of Education, Chongqing 400065, China.

²Department of Genetics, Development and Cell Biology, Iowa State University, Ames, IA 50011, USA.

³Chongqing Agriculture Science Institute, Chongqing 400055, China.

Accepted 26 June, 2011

In this work, an agent-based functional-structural model of growth simulation for Orange tree is presented. This simulation model is named ORASIM (ORange tree SIMulation). In ORASIM, functions such as carbon/water acquisitions, expenses and their dynamics are embedded into individual metamer/root agents with detailed geometries and 3D shapes. The organization of metamer/root agent's nested-list forms a growing, three-dimensional orange tree structure. After model parameterization using field data of orange tree growth, main features of functioning on whole tree level, that is, morphological and physiological responses to environmental heterogeneity have been investigated. It demonstrated that, using ORASIM, the phenotypic plasticity of orange tree can be fully emerged from interactions between agents. Moreover, the outputs of ORASIM, such as the characters of shape, branch pattern and other physiological features, show a good agreement between the simulation and the real growth orange trees.

Key words: Emergent property, metamer, autonomous agents, digital orange tree, simulation.

INTRODUCTION

The variation of structure and complexity of physiology of trees, as well as their phenotypic plasticity in response to environmental heterogeneity (Bradshaw, 2006; Zhang and Midmore, 2005), have attracted attention to devise approaches to capture and simulate these complexities in different ways. During the long history of tree growth modeling (Vos et al., 2009), many kinds of tree models focusing on different aspects in terms of function and structure have been developed, for example, some models utilize statistical (Botkin et al., 1972), empirical equations (Martin and Ek, 1984; Robinson and Ek, 2000), some are combined with pipe theory (Shinozaki et al., 1964), some models focus on a tree's physiological growth processes (Mäkelä and Hari, 1986; Weinstein and Yanai, 1994; McMurtrie and Landsberg, 1992; Landsberg and Waring, 1997; Landsberg, 2003), while others focus

on the branching pattern (Hallé et al., 1978; Jaeger and De Reffye, 1992; Prusinkiewicz and Hanan, 1989, 1992; Kurth, 1994, 2000; Godin et al., 1999; Godin, 2000; Prusinkiewicz, 2001) of the tree crown as well as the root system (Vrugt et al., 2001; Coleman, 2007). Considering tree growth models ranging from simple to extremely complicated, physiological processes and structural morphology are two critical properties that may and cannot be ignored. Both process-based tree models (PBTMs) and morphological modeling approaches undergo limitations (Prusinkiewicz, 2004). These two basic approaches are, however, to a certain degree complementary and can be combined into a better modeling approach by reducing the limitations of each. Such is what is called functional-structural tree modeling (FSTM) (Prusinkiewicz, 2004; Perttunen et al., 1996, 1998, 2001; Sievänen et al., 2000; Rauscher et al., 1990; Host et al., 1990; Reffye et al., 1995, 1997, 2003; Yan et al., 2004; Wang and Jarvis, 1990). The functional-structural tree models bridge the gap between PBTMs

*Corresponding author. E-mail: quhc@cqupt.edu.cn.

and tree architecture models by depicting an accurate 3-D perspective of plants as an aid to analyzing plant behavior. Most FSTMs represent a tree as a collection of elementary units such as bud, leaf, internode, branching point, and stem segment (Perttunen et al., 1996; Rauscher et al., 1990; Godin et al., 1999), more common in modular perspective, the metamer (Room et al., 1994; Sterck et al., 2005; Sterck and Schieving, 2007). In such models, both morphological structure and physiological processes can be integrated in the same unit. These modular designed FSTMs also have the obvious advantages of enhanced speed of simulation due to the capability of parallel computing.

Nevertheless, most FSTMs simulate tree growth using specific growth rules (Sievänen et al., 2000, 2004; Perttunen et al., 1996, 1998, 2001), for example, using the manually designed L-system to control the iteration of elementary units. Growth rule design for a specific type of tree is a time-consuming work. Not to mention that different types of tree have different branching patterns (Barthélémy and Caraglio, 2007). All individual trees in nature are distinct entities exhibiting behavior typical of all complex organisms (Trewavas, 2005) which development held in balance by complex cause-effect interactions as regards the internal physiological process and external environmental heterogeneities. These complex behaviors have no identifiable centers of tactical, as opposed to strategic, control. Traditional FSTMs aforementioned cannot model these emergent features effectively (Qu et al., 2007). New modeling paradigm, such as the teleonomic approach that can emerge complex behaviors (Breckling et al., 2005) of tree development from simple and “bottom-up” perspective (Railsback, 2001) without loss of reality is a considerable option.

In recent years, tree models have been increasingly concerned over emergent properties of tree growth. A CA (cellular automata) based simulation of plant growth and competition for resources (Colasanti and Hunt, 1997; Colasanti et al., 2001; Hunt and Colasanti, 2007) and the ALMIS (Eschenbach, 2005) are both using the teleonomic modeling approach to reproduce the emergent properties (that is to say, growth and phenotypic plasticity) on global plant level through the interactions from individual organs. However, the limitations due to rough-organ design make them difficult to integrate complex knowledge and mimic the intelligent behaviors of tree growth. Moreover, the coarse diffusion approach to carbon transport in the ALMIS and the primitive 2D simulation of plant in the CA-based model also are shortcomings that need to be improved. An object-oriented FSTM GRAAL (Drouet, and Pagès, 2003, 2007) has been developed to simulate and analyze the interactions between morphogenetic processes and assimilate partitioning during the vegetative development of individual plants. Physiological and morphological knowledge is formalized at the organ level. Main features of plant functioning have been reproduced (e.g., kinetics

of root/shoot ratio for carbon, changes in priority between organs and plant plasticity to carbon availability) at the whole plant level. Another metamer-based FSTM (Sterck et al., 2005; Sterck and Schieving, 2007) was developed to explore how light might influence the ontogenetic patterns in three-dimensional (3-D) growth of trees. However, both GRAAL and model proposed by Sterck et al. (2005) did not use the pure distributed (individual) modeling approach, instead, the empirical carbon allocation and pipe theory that need global operations were incorporated.

This paper aims to present the functional and structural features of the agent-based model ORASIM for orange tree growth, and to test the effect of variable resource captures (for example, photosynthesis, and water uptake from soil) on yields and other biological properties for orange tree. Moreover, this work needs to examine the tree branching structure resulting from meristem state transitions defined in individual metamer agents. Most important, the main goal of this work is to illustrate the phenotypic plasticity (that is, response to environmental heterogeneity) emerged at the global tree level due to locally formalized knowledge at metamer/root level.

MODEL DESCRIPTION

Simulation framework

Figure 1 shows the schematic organization of the simulation framework. Three components were prepared as input: (1) An orange tree for initial stage, including topological and geometrical characteristics of metamers (roots) as well as parameter settings for the simulation. The orange tree growth begins with a very simple tree structure of a metamer in above-ground virtual environment with attached apical and axillary buds, and a connected root segment in below-ground virtual environment. (2) The real weather data file including solar radiation density and air temperature recorded every ten minutes according to Real Solar Time (RST) at the field site (Nan'an district of Chongqing municipality in southwest mainland China, 28° 06'N, 105° 27'E, 226 m altitude). (3) The branching pattern for orange trees extracted previously using automation methods such as image processing and pattern recognition (Qu et al., 2009).

The simulation consists of three loops and takes an initial orange tree, weather data and pre-extracted branching pattern as input. The first loop is the photosynthesis cycle with an interval of 30 min (area A with cyan background). The second loop is the physiological process cycle repeated hourly (area B with pink background). The third loop is the growing season cycle indicated by area C with yellow background. Two reasoning procedures are executed by each metamer agent to optimize internal carbon allocation among organs and maximize light interception, denoted by rectangles with grey background. Bud fate is determined by a function with parameters p_c (carbon availability), p_{bro} (branching order), p_{gs} (growth stage, vegetative or reproductive growth) and p_{tmp} (air temperature).

The simulation time step is the time period for an individual cycle of the process being modeled. The orange tree simulation applies three nested time steps: a photosynthesis time step, a physiological time step and a growing season step. As shown in Figure 1, the first loop is responsible for intercept radiation and photosynthesis (water

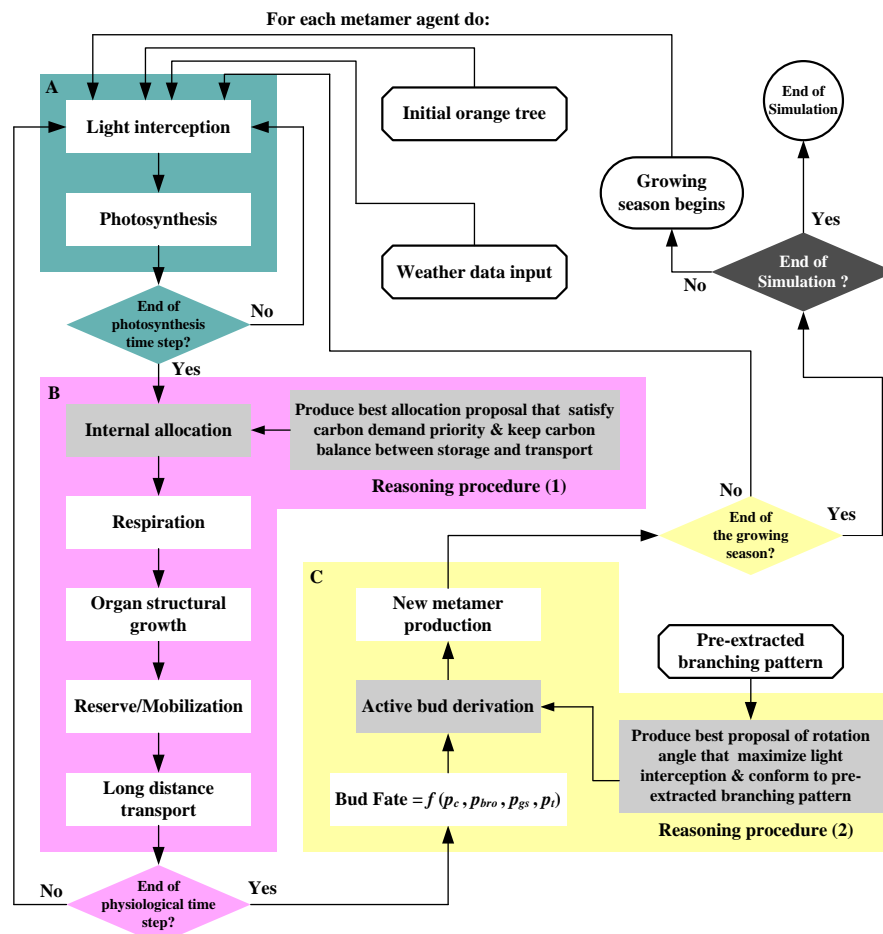


Figure 1. Schematic description of the simulation platform ORASIM.

uptake) every 30 min. The second loop is hourly based. It handles metamer (root) level carbon allocation among internal organs (internode, apical and axillary buds and optional fruits) using reasoning mechanism, executes physiological process such as respiration, carbon reserve and mobilization, axial and radial growth, as well as, long distance carbon transport. The growing season step mimics the natural annual cycle of orange tree growth. In growing season step, the active apical or axillary bud whether or not can produce a new metamer is codetermined by air temperature, carbon availability, branch order and growth stage of parent metamer. Moreover, the rotation angle denoted by the azimuth (that is, the phyllotaxy) and the inclination angle is computed optimally to maximize the radiation interception and, simultaneously, conform to angle distribution defined by pre-extracted branching pattern.

At the end of every 24 physiological time cycles (an interval of one day), the OpenGL-based 3D graphic engine scans individual metamer (root) agents using the breadth first approach to interpret their topology and geometry to 3D graphics by reading their status (including both morphological and physiological data). The shapes of individual organs in metamer are represented by predefined Bézier-surface-based mesh objects which are stored in an organ mesh library. The graphic engine with organ mesh library is similar as the Turtle interpreter implemented in L-Studio (Prusinkiewicz et al., 2004). Moreover, the graphic engine also serves as an absolute coordinate locator since agents are connected through relative coordinates. This service is provided via message exchange.

The simulation outputs are the daily results of the components of the orange tree carbon balance, that are photosynthate in total, respiratory losses, structural and non-structural (reserve) dry matter production, carbon solute status (concentration and turgor pressure) in xylem and resulting dynamics in orange tree structure (that is, number of organs, their dimension, topological and geometrical relationships, etc.).

The program of the simulation platform ORASIM was coded in Visual C++ language. Orange tree metamers and roots are constructed as intelligent agents with their in-built 3D geometry and function. A simulation engine (Agents Kernel) in the heart of the program deals with agent status and reasoning procedures as well as climate parameters to run the simulation at each time step. The Agents Kernel provides the runtime environment such as memory management, communication services as well as, geometric mapping, etc., for the metamer agents. The development of orange tree is modeled as the evolution of agents as well as their interactions in a virtual environment composed of discrete finite elements, called voxels (Figure 2) (Qu et al., 2010).

Metamer agent

Geometry and function

In ORASIM, the above-ground part of an Orange tree is composed of nested-list metamers, which are modeled as individual intelligent

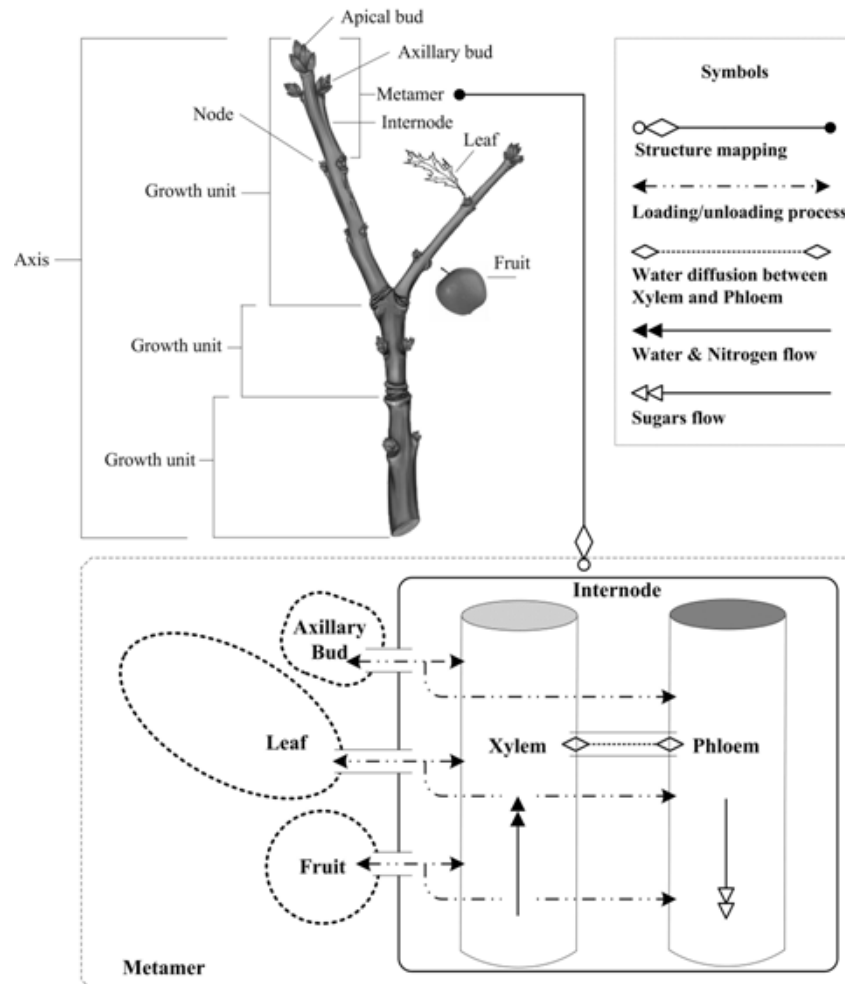


Figure 2. Physiological structure of metamer agent.

agents consisting of internode, petiole and leaf-blade, apical and axillary buds as well as possible fruits (Figure 1) (Qu et al., 2010). Metamer connects to its parent at its base with relative rotation angle. The geometry of metamer agent (used to support 3D graphic rendering according to its physiological status) is given in both schematic diagram (Figure 4) (Qu et al., 2010).

Each metamer agent possesses functional structure (Figure 2) to perform physiological processes in response to environmental heterogeneity. The metamer agent is designed as modular pattern. The Message-based loosely coupled architecture makes every part can be adapted, replaced or otherwise improved without directly affecting other modules. Each metamer agent consists of (Figure 3) (Qu et al., 2010): a sensor to perceive environmental stimulations (for example, light, temperature and water, etc.) and receive messages sent from neighboring metamer agents, an effector to execute physiological rules and send messages to neighboring agents, an interface of user operations to receive commands or messages (for example, command of pruning) from control panel of ORASIM, a communication module to handle and parse input/output messages, a memory for storing data of state variables and controller for executing actions as well as regulating access to the memory, a short-term planner and an arbiter to produce and select best proposals of internal carbon allocation and rotation angles for newly produced metamers.

Transpiration

The process of transpiration conducted by leaf leads to water potential gradients that drive water flow from soil to leaf cells. The transpiration rate per physiological step of leaf (with semimajor axis a , and semiminor axis, b) can be given as (Gao et al., 2002):

$$T_r = \pi ab \frac{(g_0 + k_{\omega\rho} I_s) d_{vp}}{1 + k_{\rho g} d_{vp}} \quad (1)$$

Where g_0 is the stomatal conductance at dark with 100% relative humidity. I_s is the photosynthetic active radiation (PAR), $k_{\omega\rho} = \omega/\rho$ is a parameter defined as changes in stomatal conductance induced by unit change in PAR, hence signifying the sensitivity of stomatal conductance to photosynthetic activities, ω ($\text{kPa mmol}^{-1}\text{m}^2\text{s}$) is a constant coefficient describing the sensitivity of osmotic potential to PAR and ρ ($\text{kPa mmol}^{-1}\text{m}^2\text{s}$) is elastic modulus of guard cell structure (Dewar 1995). $k_{\rho g} = 1/(\rho g_z)$ is a parameter signifying the sensitivity of stomatal conductance to vapour pressure deficit. g_z is a soil-to-leaf conductance coefficient and d_{vp} is the relative vapour pressure deficit defined as absolute vapour pressure deficit divided by atmospheric pressure.

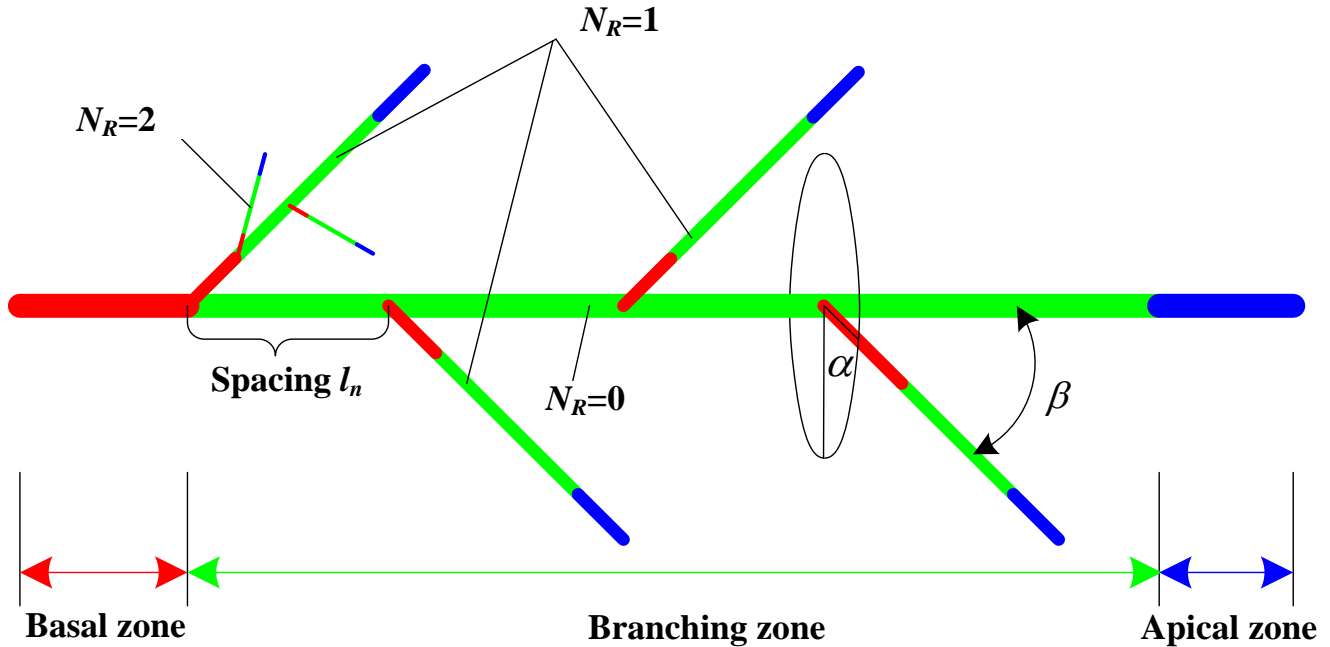


Figure 3. Schematic description of root structure. N_R : root branch order; α : azimuth angle with respect to parent root; β : inclination angle with respect to parent root.

Carbon economy

Light interception and photosynthesis: The process of light interception and photosynthesis provide estimates of carbon gain for the simulated orange tree as a function of climatic parameters and the physiological state of the leaves. The photosynthetic active radiation I_s consists of direct radiation (I_{dir}) and diffuse radiation (I_{dif}) according to the relationship between measured and potential global radiation (Nygren et al., 1996; Weiss and Norman, 1985):

$$I_s = I_{dir} + I_{dif} \tag{2}$$

The direct radiation is produced by the solar ray from sun passing directly through the atmosphere without any scattering. A solar ray is considered a source vector that originates at the solar position $H_0(x_0, y_0, z_0)$ in the upper hemisphere of the virtual environment. Solar position defines the direction of the direct solar ray. The diffuse radiation is denoted by photon flux scattered in the atmosphere due to contact with dust and water vapor. Every leaves in metamers can receive diffuse radiation which scattered uniformly from all directions of the visible hemisphere.

Assume that the centroid of a leaf has the position of $H(x, y, z)$ with azimuth α and inclination β with respect to the base of metamer, giving the incidence of sun light $R_{dir}(\theta, \varphi)$ with azimuth angle θ and elevation angle φ , the direct photon flux density I_{dir} can be calculated as a function of the relative geometry between the solar ray direction and the leaf orientation:

$$I_{dir} = (R_{dir} / \sin \varphi) * |\cos \beta * \sin \varphi + \sin \beta * \cos \varphi * \cos(\alpha - \theta)| \tag{3}$$

Where R_{dir} is the incident direct radiation and the relationship between the position of leaf and the solar position satisfy:

$$\begin{pmatrix} x \\ y \\ z \end{pmatrix} = \begin{pmatrix} x_0 \\ y_0 \\ z_0 \end{pmatrix} + \mu \begin{pmatrix} \sin \theta / \tan \varphi \\ \cos \theta / \tan \varphi \\ -1 \end{pmatrix} \tag{4}$$

Where μ is the variable parameter of the equation of the straight line. Leaves in canopy always cast shadows. In such case, the irradiance following the direction of solar ray is decreased, that is, multiplied by a shading factor (the probability that a leaf is sunlit) γ computed by Beer's law:

$$\gamma = \exp\left(-V * \frac{h}{2 \cdot \sin \varphi}\right) \tag{5}$$

Where V is the total number of leaves in the canopy, h is the height of the orange tree.

Regarding diffuse radiation, the upper sky hemisphere is divided up into m solid angle sectors in horizontal direction. Each sector i corresponds to directions with elevation φ_i and azimuth θ_i . Assuming that the diffuse incident radiation conforms to an isotropic distribution (Walsh, 1961), and considering the extinction coefficient (Goudriaan, 1977) e according to Beer's law:

$$e = \frac{2}{1 + 1.6 \sin \varphi} * \frac{1 - \sqrt{1 - \sigma}}{1 + \sqrt{1 - \sigma}} \tag{6}$$

The diffuse photon flux density I_{dif} coming from each sector i can be written:

$$I_{dif} = \sum_{i=1}^m e * (R_{dif} / \sin \varphi_i) * (\sin^2(\varphi_i + \beta / 2) - \sin^2(\varphi_i - \beta / 2)) * (\theta / \pi) \tag{7}$$



Figure 4. Pictures of orange trees growing in field site.

Where σ is the scattering coefficient of leaves, i.e. the sum of leaf reflectance and transmittance ($\sigma \approx 0.2$ for photosynthetically active radiation), R_{diff} is the incident diffuse radiation above the simulated tree.

Giving the photosynthetic photon flux density I_s at the centroid of each leaf, one of the simplest photosynthesis approach (Le Roux et al., 2001) usually used in tree growth models is to compute the photosynthetic rate P as the product of the unshaded photosynthetic rate P_{max} , the photosynthetic photon flux density I_s intercepted by leaf and the production capability of the leaf $f(BioM_L)$ (Mäkelä and Hari, 1986; Deleuze and Houllier, 1995; Mäkelä, 1997), as well as, the accelerating effect of the air temperature T and the inhibition effect of the current carbon status CM_x :

$$P = \frac{P_{max} * I_s * f(BioM_L) * \tau(tmp)}{1 + (CM_x / k_h)} \quad (8)$$

Where $BioM_L$ is the biomass of the leaf and the function $f(*)$ is the widely used negative exponential function (similar to $f(x) = 1 - \exp(-x)$) with the value range from 0 to 1. The parameter k_h is the inhibition factor influenced by accumulated photosynthate in the metamer. The function $\tau(*)$ is the temperature effect, it has the form:

$$\tau(tmp) = \min\left(\frac{tmp}{25^\circ C}, 1\right) \quad (9)$$

Internal carbon allocation: As an autonomous growth based orange tree model, it is necessary for a metamer to deal with carbon production and internal consumption prior to tree level partition by means of long distance transport. The internal carbon consumption of metamer includes respiration, growth and reserve for individual organs, for example, internodes, leaves, buds and possible fruits. During the lifetime, the goal of each metamer agent is to keep balance between carbon production, consumption and storage, as well as, provide carbon supply as much as possible to other parts of the tree. This goal make a metamer agent might avoid abortion and live as long as possible (refer to senesce or death rules), and the same holds for the entire tree. However, with various growth stage and environmental conditions, each organ has different carbon demand priority, sink strength and reserve/mobilization ratio. To design how metamer agents determine the proposal of internal carbon allocation in each physiological time step, we reason as follows:

Let $CM_x(t)$ be the available carbon content of the metamer carbon pool at time step t . After two cycles (times) of photosynthesis, photosynthate $2\Delta t * P(t)$ produced by leaves is added to $CM_x(t)$ where Δt is the length of photosynthesis time step (that is, 30 min) which is half of the time of physiological step (Figure 1).

Prior to constructive carbon consumption, a large amount of carbon need to be used for respiration (Sprugel and Benecke, 1991). Carbon consumption in plant respiration can be divided into two

Table 1. Organ dimension change due to axial and radial growth.

Organ dimensions	Equations
New volume of internode	$V_I(t+1) = \frac{G_I(t) + BioM_I(t)}{D_I} \quad (11)$
New radius of internode	$r_I(t+1) = \sqrt[3]{\frac{G_I(t) + BioM_I(t)}{D_I \pi R_I}} \quad (12)$
New height of internode	$h_I(t+1) = R_I * r_I(t+1) \quad (13)$
New area of leaf-blade	$S_L(t+1) = \frac{G_L(t) + BioM_L(t)}{D_L} \quad (14)$
New semimajor axis of leaf-blade	$a(t+1) = \sqrt{\frac{G_L(t) + BioM_L(t)}{D_L \pi R_L}} \quad (15)$
New semiminor axis of leaf-blade	$b(t+1) = R_L * a(t+1) \quad (16)$
New volume of fruit	$V_F(t+1) = \frac{G_F(t) + BioM_F(t)}{D_F} \quad (17)$
New radius of fruit	$r_F(t+1) = \sqrt[3]{\frac{3(G_F(t) + BioM_F(t))}{4\pi D_F}} \quad (18)$

components: the growth respiration and the maintenance respiration (4). The former concerns the energy requirement of the biosynthesis of structural plant components, while the latter is the energy required to maintain a living organism in steady state. For simplicity concern, the proposed orange tree simulation has used the one-component approach, that is, maintenance respiration $M(t)$ is calculated as a function of the weight of biomass of each organ in metamer (Takenaka, 1994; Prentice et al., 1993) and a function of temperature effect (Amthor, 1984):

$$M(t) = \eta^* (BioM_L + BioM_I + BioM_{AP} + BioM_{AX} + BioM_F) * \tau(T), \quad (10)$$

Where η is the coefficient specific respiratory costs (Sprugel and Benecke, 1991) for both maintenance and growth. The effect of temperature on respiration (Amthor, 1984) is computed by the function τ^* which has the form similar to equation 8.

After accounting for the respiration costs the available carbon is allocated to individual organs for axial and radial growth. Generally, the carbon demand for organ growth is quantified as the genetic Potential Growth Rate (PGR) of a sink (Genard et al., 2008), that is, the maximum growth rate achieved by the growing organ in optimal environments. The PGR determines the sink strength which is the respective ability of different sinks to get available carbon (Lacointe, 2000). The sink strength of individual organs with age is a function of the accumulated temperature (Way and Oren, 2010), and can be represented reasonably well by a Gompertz curve (Marcelis et al., 2002).

The partition among individual organs in metamer is not only related to their sink strength but also to their priority which has totally different scenario due to different growth stages. When the available carbon is more than the total demand of organs, each organ is fully satisfied and grows at its PGR, and the excess supply goes to the reserves in the form of starch and consequently photosynthesis is inhibited. In case of shortage, a decision has to be made is that how much carbon each organ will get. The solution used by the metamer was the so-called "hierarchical" approach (Yin

and van Laar, 2005), the organ with the highest priority is "fully served" first, and only then the organ with the next priority level is considered, and so on. The generally accepted sink priority order (Wardlaw, 1990; Williams, 1996) is: fruits (seeds) > apical and axillary buds > leaves = internode. When individual organs obtain amount of carbon $G(t)$ for axial and radial growth, giving genetic parameters density D their new dimensions including volume, height and radius can be respectively calculated (Table 1).

Trees usually store some amount of carbon in the form of starch when carbon available in excess of the active growth demands. These reserves act as supplemental sources to provide carbon compensation when current photosynthesis is not sufficient to meet the carbon requirement for a period of time (usually in spring, during the intense growth of new internodes and leaves) (Le Roux et al., 2001). For biological reasons, the available carbon content of organ cannot drop below a given threshold. Technically, we control carbon reserve and mobilization on metamer level other than the entire tree. A dynamic coefficient χ called carbon saturation deficit is employed to control the carbon status of a metamer into a steady state. Therefore when carbon available $CM_X(t)$ exceeds this threshold, the reserve process is activated to store amount of χ into starch pool S . On the contrary, the mobilization process is activated to hydrolyze starch as much as possible for compensation. Through the internal carbon allocation for respiration, growth, reserve and mobilization, the content of the metamer available carbon pool at physiological time step $t+1$ can be written:

$$CM_X(t+1) = CM_X(t) + 2\Delta t P(t) - M(t) - G(t) \pm \chi \quad (19)$$

Long distance transport: In higher (vascular) plant, the long distance transport of carbon between source and sink organs can be viewed as the results of carbon motion (flux) between any direct neighboring cells, which join into sieve-tubes that form the vascular system (Lincoln, 2004). In a discrete approach, the long-distance transport in xylem and phloem using pressure-flow hypothesis (Thompson and Holbrook, 2003) are decomposed into nutrients

interchange between direct neighboring internodes, in which the xylem and phloem segment join into tubes that form the complex vascular system of higher plant. Assume in each internode of metamer and root, the xylem segment contains W_x mol water, while the phloem segment contains W_p mol water and CM_x mol carbon. In an approximate manner, we compute the hydrostatic pressure in xylem segment as:

$$P_x = \frac{\varepsilon \cdot W_x}{\pi R_x^2 h_l} \quad (20)$$

Where ε is the cell elastic modulus, R_x and h_l are respectively the radius and height of xylem segment. Because the xylem sap has a very low solute concentration which we shall ignore, so there is no osmotic component to its total water potential. Therefore the water potential in xylem is:

$$\Psi_x = P_x \quad (21)$$

Similarly, the hydrostatic pressure in phloem segment is:

$$P_p = \frac{\varepsilon \cdot (W_p + CM_x)}{\pi R_p^2 h_l} \quad (22)$$

Where R_p is the radius of phloem segment. For the sake of simplicity, we ignore the thickness between xylem and phloem. The water potential in phloem is:

$$\Psi_p = P_p + \Pi_p, \quad (23)$$

Where Π_p is the osmotic potential of solution of carbon, it is computed as:

$$\Pi_p = -R \times T \times \frac{CM_x}{W_p + CM_x} = -R \times T \times \rho_s \quad (24)$$

Where R is the universal gas constant and T is the absolute temperature, and ρ_s is the carbon concentration. The water osmosis between xylem and phloem resulted from the difference of water potential, according to Fick's first law of diffusion, the water content exchanged in osmotic process is:

$$Q_{w, xp} = \frac{1}{r_{xp}} (\Psi_x - \Psi_p) \quad (25)$$

Where r_{xp} is the apoplastic pathway resistance between xylem and phloem. According to Münch pressure-flow hypothesis (Minchin et al., 1993), solute fluid motion between any two direct connected internodes is driven by the hydrostatic pressure difference. Therefore, in xylem and phloem, the water and carbon solute flow exchanged between internode i and j are respectively given as follows:

$$Q_{x, ij} = \frac{1}{r_{x, ij}} (P_{x, i} - P_{x, j}) \quad (26)$$

$$Q_{p, ij} = \frac{1}{r_{p, ij}} (P_{p, i} - P_{p, j}) \quad (27)$$

Where $r_{x, ij}$ and $r_{p, ij}$ are respectively the average resistance of xylem and phloem segment between internode i and j (Thompson and Holbrook, 2003).

In simulation, we assume that the water and carbon fluids are incompressible, which require volume conservation for every internode. This means that the sum of the fluxes in one internode and all its neighbors $\Gamma(i)$ (including both parent internode and child internodes) should vanish to satisfy volume conservation principle:

$$\sum_{j \in \Gamma(i)} Q_{x, ij} + Q_{w, xp} = 0, \quad (28)$$

$$\sum_{j \in \Gamma(i)} Q_{p, ij} - Q_{w, xp} = 0. \quad (29)$$

Therefore, the new hydrostatic pressure in xylem and phloem segment of internode i at simulation step $t+1$ will be updated by:

$$P_{x, i}(t+1) = \left\{ \sum_{j \in \Gamma(i)} \frac{1}{r_{x, j}} P_{x, j}(t) + \frac{1}{r_{xp}} [\Pi_p - P_{p, i}(t)] \right\} / \left(\frac{1}{r_{xp}} + \sum_{j \in \Gamma(i)} \frac{1}{r_{x, j}} \right) \quad (30)$$

$$P_{p, i}(t+1) = \left\{ \sum_{j \in \Gamma(i)} \frac{1}{r_{p, j}} P_{p, j}(t) - \frac{1}{r_{xp}} [\Pi_p - P_{x, i}(t)] \right\} / \left(\frac{1}{r_{xp}} + \sum_{j \in \Gamma(i)} \frac{1}{r_{p, j}} \right) \quad (31)$$

Then the new value of carbon and water content in phloem and xylem at simulation step $t+1$ can be calculated according to the hydrostatic pressure computation (Equation 21):

$$CM_{x, i}(t+1) = \frac{1}{\varepsilon} P_{p, i}(t+1) \pi R_p^2 h_l - W_p(t) \quad (32)$$

$$W_p(t+1) = \frac{1}{\varepsilon} P_{p, i}(t+1) \pi R_p^2 h_l - CM_x(t+1) \quad (33)$$

$$W_x(t+1) = \frac{1}{\varepsilon} P_{x, i}(t+1) \pi R_x^2 h_l \quad (34)$$

At the end of each physiological time step, a metamer/root agent send a message to its entire neighborhood $\Gamma(i)$ to request their available carbon and water content, radius and length of xylem and phloem segment. Then this metamer/root agent computes and updates its new available carbon and water content according to the pressure-flow hypothesis. This computing process is implemented by a separate thread and executed in parallel mode similar to the cellular automata, where each cell is analogous to the individual metamer/root agent.

New metamer production

The growth of orange tree begins from each active apical and axillary bud. Each bud could develop into a new branch. During a single growing season, only one bud of each branch is set as active and serves as the basis for deriving a new metamer in the next step. All other buds are set as dormant with respect to bud derivation. These dormant buds do not become active until the

beginning of the next growing season. Which bud in a branch will be set as active in a growing season is determined by the probability of bud fate ($B_{PActive}$), giving as the form:

$$B_{PActive} = f_1(CM_X) * f_2(N_M) * f_3(gS) * f_4(tmp) \quad (35)$$

Where f_i are empirical multiplier functions with the value ranges from 0 to 1 (Dizès, 1998).

The bud fate depends on the probabilities that relate to the metamers available carbon content, metamer branch order, metamer growth stage (vegetative or reproductive) and air temperature. First, the value of f_1 is set to 1 for this metamer if it has accumulated enough carbon for the production of a new metamer (infancy) including its child organs such as leaves, internode as well as attached buds. Otherwise, the value of f_1 is set to 0. The threshold value of carbon needed for producing a young metamer is calculated by the product of the total biomass of the metamer and a user configurable coefficient λ between 0 and 1. Second, the branch order N_M affects the decreasing probability of bud activation as a constant fraction per branch order (Sterck et al., 2005). Third, the effect of growth stage is the function of simulation step that is roughly divided into the stage of vegetative growth and the reproductive growth (Wright, 1989). In the vegetative growth stage, the apical bud has the priority to be activated than the axillary bud, and on the contrary, the axillary bud has the priority than the apical bud in the reproductive growth stage. The apical dominance of tree growth is guaranteed via the control of second and third function. Finally, bud growth is driven by air temperature. Therefore, the effect increases linearly with the amount of accumulated temperatures above the threshold of 4.5°C (Richardson et al., 1974).

In a growing season, all buds, both active and dormant, create new leaves each time buds are created. The active bud creates a new metamer having relative rotational angle (azimuth and inclination) with respect to the parent metamer. Prior to the new metamer production, the relative rotational angle need to be calculated to make sure that the new leaf-blade on the new metamer will hold the best position to maximize light interception, and simultaneously, has to satisfy the pre-extracted branching pattern of orange tree.

Three- and four-year-old orange trees were sampled in the open growth plantation (field site) and an automatic method (Qu et al., 2009) was used to obtain the branching pattern. Measurement of orange tree structure included branch base diameter, branch number and bifurcation angle, internode segment diameter, and segment length. The data of branching pattern were organized as types (groups) of growth unit (GU) sharing similar characteristics, as well as probabilities of transition among these GU types. The partitioning of GU types reveals the hidden states (Maillette, 1990) that indicate different stages of differentiation in the meristems. Moreover, the transitions among GU types imply the changes of geometry and topology through the plant structure referred to as morphogenetic gradient (Barthélémy and Caraglio, 2007). The transitions define the distribution of azimuth (Φ_α) and inclination angle (Φ_β) between parent GU and its children. When a bud prepare to birth a new metamer, which type of GU it belongs to has to be made clear according to the features of parent metamer. Then the possible range of relative rotation angle can be specified. Therefore, the best azimuth and inclination of leaf-blade with respect to the base of new metamer that can maximize the light interception can be calculated as:

$$\alpha_{\max}, \beta_{\max} = \arg \max_{\alpha \sim \Phi_\alpha, \beta \sim \Phi_\beta} (I_{dir} + I_{dif}) \quad (36)$$

Where I_{dir} and I_{dif} are respectively the direct and diffuse photon flux density calculated by Equations 2 and 6.

Senesce (death)

Senesce rule is also considered for each metamer at every physiological time step. The probability of metamer death is determined by metamer age, free and reserve carbon content, water deficit and atrocious air temperature:

$$M_{PDeath} = f_1(Age) * f_2(CM_X) * f_3(W_X) * f_4(tmp) \quad (37)$$

Where f_i are empirical multiplier functions with the value ranges from 0 to 1 (Dizès, 1998). These functions evaluate whether the metamer has passed its maximum age, its available carbon content is negative (metamers respiration exceeds the sum of net photosynthesis production and carbon transported from other metamers), and it suffers water stress as well as, the air temperature oversteps the range between lowest and highest threshold. Once a metamer dies, all its child metamers will be removed immediately.

Root agent

Elongation and branching

Root agents have similar properties as metamer agents in terms of agent function and physiological rules. However, roots have different growth patterns in comparison with metamers in shoot system from the perspective of geometry, for example, the lateral branching (Figure 3). Lateral roots initiate from internal cells of the pericycle (van den Berg et al., 1995). Initiation occurs in the late cell elongation/early cell differentiation zone, in pericycle cells that are partially to fully differentiate. Thus there is no detached meristem. Generally, a root produces child roots with successive order at the branching zone with certain spacing (Jourdan and Rey, 1997), that is, each new child root is created if and only if the branching zone produces an elongation l_n . In ORASIM, we use an elongation function (Pages, 1999) to control the growth of branching zone:

$$\lambda_i(t) = k_i \left(1 - \exp\left(-\frac{r_i}{k_i} t\right)\right) \quad (38)$$

Where $\lambda_i(t)$ is the branching zone elongation of root with branch order i , t is the physiological time step, k_i is the maximal length of the root and r_i is the growth rate (speed) which is determined by the genetic Potential Growth Rate (PGR) R_{max} (Riedacker, 1976) the available carbon CM_X and the stimulation of soil temperature tmp (Cooper, 1973):

$$r = R_{max} f_1(CM_X) f_2(tmp) \quad (39)$$

Where f_i are empirical multiplier functions with the value ranges from 0 to 1.

The spatial distribution of roots in growth is primarily determined by water and nutrient potential (Chikushi and Hirota, 1998). When the elongation of branching zone reaches the threshold l_n , a new root with higher branch order will be produced. The growth direction of this new root is driven (attracted) by water concentration in soil environment (Smit et al., 2000). Therefore, the relative rotation angles (both the azimuth and inclination) which connect the new root to its parent should be calculated in order to lead this root growth towards the direction with highest water concentration (Theseira et al., 2003). Nevertheless, the rotation angles have to be restricted into specific range so that the growth pattern of the whole root system (Coleman, 2007; Mulia and Dupraz, 2006) can be

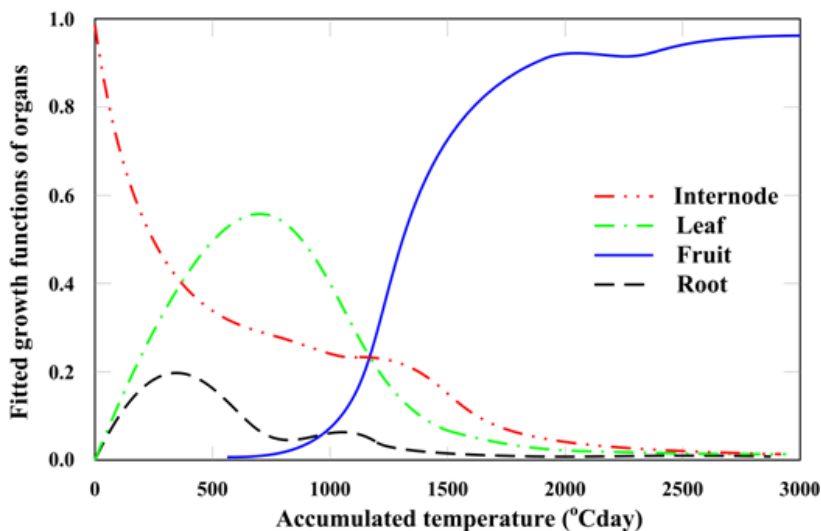


Figure 5. Fitted growth functions (relative growth rate, RGR) for organs in metamer and root.

maintained. Root rotation angle computation is similar to the procedure of best angle chosen for metamer agent.

Water uptake

In ORASIM the orange tree uptake of water from soil is mainly determined by the root spatial distribution in the soil, atmospheric water demand due to leaf transpiration and the availability and potential of soil water as well as the potential growth rate of root (van den Berg and Driessen, 2002; van den Berg et al., 2002). The root water uptake rate per physiological step is written:

$$W_U = r \cdot (1 - \exp(-\frac{BioM_R}{\Psi_x - \Psi_s})) \tag{40}$$

Where r is the root elongation rate. Ψ_x and Ψ_s are respectively the water potential in root xylem segment and soil voxel where the root apical zone is located, that is, $(\Psi_x - \Psi_s)$ indicates the water potential gradient between root and soil (Wang and Smith, 2004). The potential gradient is caused by water transport in xylem due to leaf transpiration taking place in the crown. $BioM_R$ is the total biomass of root including three zones.

Parameterization

The simulation result of ORASIM provides the detailed structural and physiological information about Orange tree growth under a specific environment which was configured by measured real weather data. The detailed information includes Orange tree height, foliage area, total biomass in shoots and roots. Additional information such as number of leaves, internodes and fruits are also available on request. In addition to numerical data for model results, simulation results are also presented as a visualized Orange tree. The tree visualization provides heuristic expression of the simulated results, which can be compared and validated with the visual appearance of real orange tree grown in the field site. After the experimental measurement and model parameterization, ORASIM is implemented and simulation results have to be validated. The

model validation involves the comparison of simulation results with field data acquired from different area to ascertain whether the modelling method could explain the orange tree growth mechanisms in terms of tree structural development and biomass growth.

Weather data were provided by an automated weather station (weather bureau of Nan'an district, Chongqing City, China). The weather station recorded global radiation, photosynthetic photon flux density, net radiation, wind speed, soil temperature, air temperature, air humidity, and rainfall. Photosynthetic photon flux density and temperature were used in ORASIM, and global radiation was applied for estimating direct and diffuse components of incident photon flux density. Soil water content was directly measured using a known volume of the material, and a drying oven. Volumetric water content is calculated (Dingman, 2002) using:

$$W_C = \frac{m_{wet} - m_{dry}}{\rho_w \cdot V_b} \tag{41}$$

Where m_{wet} and m_{dry} are respectively the masses of the sample before and after drying in the oven; ρ_w is the density of water; and V_b is the volume of the sample before drying the sample.

Determination of growth functions for organs was based on orange samples taken from each plot 20 times during the growing season. These sample orange trees growing in optimal environment with sufficient radiation, temperate climate and without suffering water stress as well. Every sample consisted of 1 to 18 Orange trees chosen by the distribution of their simple biometrical indicators. The organs of sample orange trees were separated and weighed. The organ growth functions (Figure 5) were fitted as the dry matter increments of individual organs between subsequent measurements.

As far as possible, initial trees and input parameters in ORASIM, such as photosynthesis, transpiration and respiration, reserve and mobilization as well as branching patterns were drawn from field data on living orange trees growing in the field site. The maximum photosynthetic rate, transpiration rates, and stomata conductance of the first fully expanded leaf near midday were measured with LI-6400 portable photosynthesis system (LICOR Biosciences Inc.). Otherwise, parameter values were taken directly from the literature.

Table 2. Four scenarios of simulated environment.

Simulated environment	Air temperature (°C)	Light intensity	Soil water capacity (%)
Optimal condition	Constant 25	Constant 20 klx	100
Low temperature	Constant 10	Constant 20 klx	100
Low light	Constant 25	Constant 10 klx	100
Water stress	Constant 25	Constant 20 klx	30

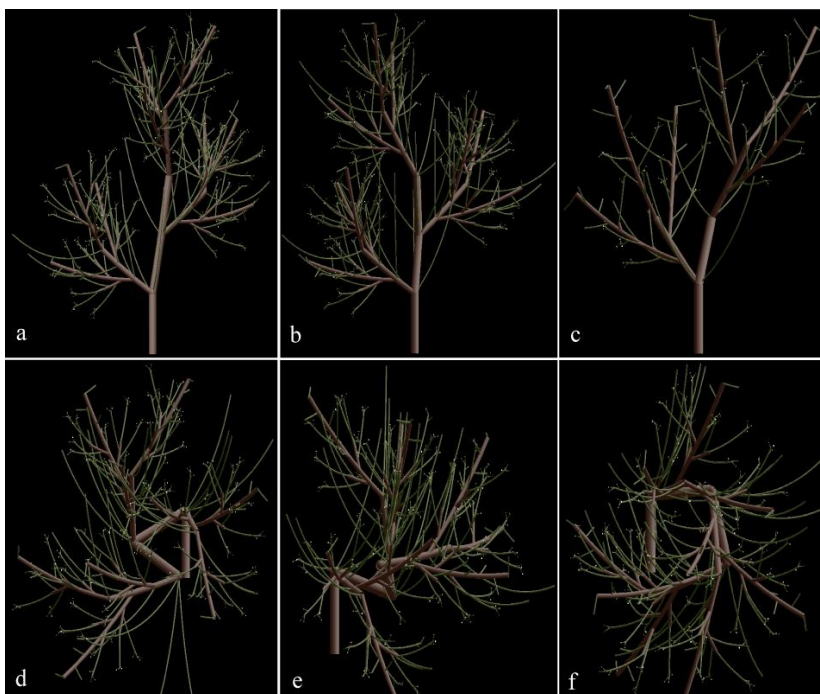


Figure 6. Simulation outputs of ORASIM: effects of control of pre-extracted branching pattern on simulated orange tree structure. The branching process of (a), (b) and (c) conform to the distribution of rotation angle specified by the pre-extracted branching pattern. Random branching was employed in the case of (d), (e) and (f).

RESULTS

In order to validate and demonstrate ORASIM's capability of simulating Orange tree growth (morphology and physiology) in response to environmental heterogeneity, simulation experiments and corresponding comparisons between measured and simulated data as well as, 3D graphics were conducted. Measured weather data and soil moisture were collected to validate ORASIM. Four virtual environmental configurations including optimal and stressful conditions were introduced (Table 2).

Morphological responses

General architecture and shape

During simulation, pre-extracted branching pattern was

incorporated into ORASIM. The branching pattern was extracted from sampled orange trees using an automatic approach (Qu et al., 2009). It consists of grouped growth units defined as hidden states which have similar statistical properties and transition probabilities among them. When a new metamer is going to be born, the possible rotation angle with respect its parent is referred to ranges defined by transitions between hidden states. Therefore, branching process with pattern control makes tree's development holding the pattern of a real one, as shown in a, b and c in Figure 6. Nevertheless, without this control, tree growth might be irregular, as shown in d, e and f in Figure 6, lacking of reality.

The comparison in terms of appearance and general shape between simulated and real orange trees has been conducted. Figure 7 shows the orange tree growing at different stage: year 2 (height 0.82 m, Figure 7a), year 3

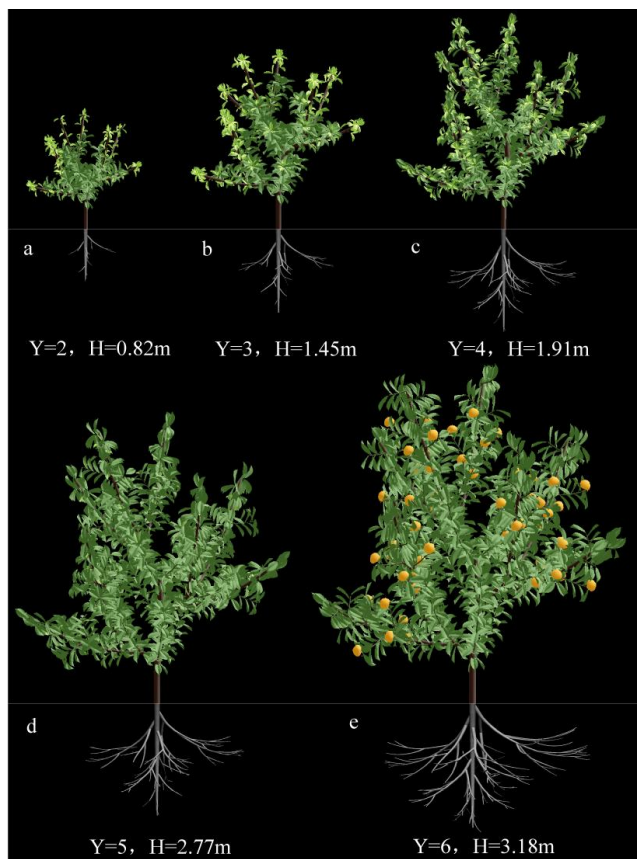


Figure 7. Simulation outputs of ORASIM: an orange tree growing in specific environment configured by measured weather data and soil moisture (2003-2009). The pictures represent growth stage (after planting) at (a) year 2, (b) year 3, (c) year 4, (d) year 5 and (e) year 6, respectively.

(1.45 m, Figure 7b), year 4 (1.91 m, Figure 7c) in vegetative growth stage as well as, year 5 (2.77 m, Figure 7d) and year 6 (3.18 m, Figure 7e) in reproductive growth stage. This simulated orange tree grown in measured weather which is the same as the real one. The results of tree height show that there is a good agreement between the simulation and field observation. From year 2 to 6, the relative error of tree height between simulation and observation are: 2.66, 1.87, 2.09, 2.15 and 3.28%, respectively.

Figure 8 shows four simulated orange trees after 6 years development under different conditions: Orange tree in Figure 8b has undergone low air temperature, orange tree in Figure 8c has undergone low light intensity and orange tree in Figure 8d has suffered water stress, while the orange tree in Figure 8a grown under optimal condition. All three orange trees underwent deficient conditions show a smaller and shorter shape than the optimal growth one. Especially the growth of the tree suffered low light was dramatically retarded.

Leaf area of these trees was 1.75, 2.52 and 3.07 m² in contrast with 4.33 m² of the optimal one. The

corresponding tree heights were respectively 2.26, 2.79, 2.88 and 3.38 m. The simulated data tally with the observations (Table 3). Moreover, the simulated height growth of these trees was closely related to the simulated total leaf area in the tree. This relation leads to that the amount of leaves existing above a certain horizontal level in a tree is always proportional to the sum of the cross-sectional areas of the stems and branches at that level, that is, the more leaves they support, the thicker the branch diameters and the longer the branch length. Since the ORASIM use fixed scale coefficient to describe the shape variation of stem, there is a positive correlation between cross-sectional area and stem length. This phenomenon is well verified by the pipe model proposed by Shinozaki et al. (1964). These authors found a direct correlation between the total cross-sectional area at any horizontal level and the leaf mass above that level.

The architecture and distribution of the root system primarily resulted from root functions in the acquisition of soil water (Fitter, 2002; Wang et al., 2006) and carbon supply from shoot system (Lynch, et al., 1996). The total root length and horizontal expansion was larger in



Figure 8. Simulation outputs of ORASIM: four 6-years-old orange trees growing respectively in (a) optimal condition, (b) low air temperature, (c) low light intensity and (d) water stress.

Figures 8a, b and c under well-watered condition than in Figure 8 d suffering water stress mainly because of more elongation of branching zone of root and greater lateral root length in the former. Drought significantly reduced the number and the total length of roots, and the total length of lateral roots. Moreover, the orange trees suffering low light and low temperature (Figures 8b and c) has less total biomass than the one grown in optimal condition (Figure 8a) because of growth being restricted (Taiz, 2004; Somma et al., 1998) due to less carbon allocation from shoot (Table 3).

Shoot phototropism

ORASIM provides the architecture of distributed intelligence for orange tree growth, that is, each metamer (leaf) and root agent can autonomously perceive local light and water gradients in sky and soil environment (as illustrated in Figure 9). This crucial infrastructure makes it possible that the ORASIM can vividly simulate the shoot phototropism and root hydrotropism, which might have significant effects on the light interception, dry matter production and yields of orange tree (Vos et al., 2009). Figure 10a shows the simulated phototropism of orange tree with structure adaptation. The fully growing form with leaf cover and fruit production of the same orange tree were also given in Figures 10b and c. In Figure 10, light was coming from top left corner of the sky, so that right-sided leaves and apical buds gradually found them in the shade. Since the carbon allocation and the activation of the shoot apical buds depends partially on the access to light intensity, only left-sided apical buds continued to

develop. Consequently, the orange tree adapted to the constraint by developing branches which are bent downwards. In contrast with our metamer movement approach, a phototropism model for cucumber canopy was developed by Kahlen et al. (2008) using a parametric L-system. Their approach directly modeled the leaf movement induced by gradients (the red to far-red ratio) in the local light environment of each leaf.

Root hydrotropism

It has been shown that the survival of terrestrial trees depends on the capacity of roots to obtain water and mineral nutrients from the soil (Filleur et al., 2005; Eapen et al., 2005). Roots growth is adapted to moisture gradient in soil is called hydrotropism. Orange tree in Figure 11 was growing in a soil environment where water is diffused from a single source located in down left corner. It can be observed how the root growth followed this specified disposition of water. Figure 11a shows the simulated procedure of hydrotropism for root system of an orange tree. Figure 11b and c also schematically show the relative position between root and water source respectively in front and top view.

Physiological responses

In addition to morphological responses, orange tree may also adapt to the environmental constraints by regulating carbon reserve and mobilization, shifting balance of carbon allocation as well as adjusting productivity. In ORASIM, such behaviors are engendered by the

Table 3. Measured and simulated orange tree attributes after growing 6 years. The number of measured orange trees growing in optimal, low light intensity, low air temperature and water stress conditions are respectively 16, 16, 17, 18.

Orange tree attributes	Measurement				Simulation			
	Optimal condition	Low light	Low temp.	Water stress	Optimal condition	Low light	Low temp.	Water stress
Height (m)	3.29±0.12	2.15±0.26	2.69±0.19	2.67±0.43	3.38	2.26	2.79	2.88
Leaf area (m ²)	4.29±0.26	1.89±0.11	2.68±0.51	3.12±0.17	4.33	1.75	2.52	3.07
Number of metamers	219±3.22	120±2.62	142±1.88	187±2.12	223	127	140	192
Number of roots	87±2.52	61±1.37	74±2.70	78±3.19	89	59	75	77
Number of leaves	661±5.17	512±4.65	588±7.29	576±6.40	673	449	527	558
Number of internodes	219±3.22	120±2.62	142±1.88	187±2.12	223	127	140	192
Number of fruits	198±2.73	72±1.81	84±4.55	32±0.64	221	65	71	21
Weight of fruits (kg)	43.02±4.05	11.24±2.31	13.15±1.78	9.73±3.22	45.76	10.25	10.43	8.31
Shoot dry matter (kg)	5.64±0.04	2.94±0.02	4.02±0.05	3.26±0.06	5.48	2.76	3.97	3.44
Root dry matter (kg)	0.83±0.07	0.16±0.03	0.31±0.02	0.72±0.11	0.95	0.22	0.28	0.39
Dry matter in total (kg)	6.47±0.12	3.10±0.09	4.33±0.10	3.98±0.16	6.43	2.98	4.25	3.83

dynamics of metamer internal carbon allocation and the pressure-flow transport which leads global carbon distribution within the whole tree. As the ultimate results of tree response to environmental constraints, simulated organ numbers, dry matter and yields on global level were listed in Table 3 by means of comparison between stressful and optimal conditions.

Effects of light intensity

Through the entire life span of tree, carbon reserve and mobilization is a mean by which trees cope with environmental hazards (Roux et al., 2001). This requires that the reserved carbon should be dynamically regulated according to the free carbon, because free carbon is the most important source for organs to deal with carbon deficit due to shading or spring growth demand (Lacointe et al., 1993). To simulate this phenomenon, each metamer or root agent can perceive the level of free carbon and automatically

release (hydrolyze) or store amounts of free carbon to keep the level of free carbon to be stable.

Typically, light intensity can dramatically affect the photosynthesis rate (Sprugel and Benecke, 1991) and consequently influence carbon dynamics on the whole tree level. Figure 12 shows the effects of light variations on total carbon content and reserve dynamics of orange tree. The weather data are average intensity of illumination measured at the field site from January, 2008 to January, 2010. When the light was lowered in winter, the orange tree underwent a global loss of carbon due to the dramatically decreased photosynthesis efficiency. Then the reserved starch was hydrolyzed to compensate carbon deficit. This behavior leads to sharp decrease of starch and slight decrease of free carbon. After the light was restored in spring and summer, the carbon productivity of orange tree recovered and the reserved starch returned to increase, total free carbon also increased as well. Result of Figure 12 shows that the simulated (lines) effects of light intensity on carbon dynamics

fitted well with the observations (symbols).

Effects of air temperature

All biochemical processes in a tree are temperature dependent, the growth of organ can only occur after a certain specific threshold of temperature accumulation has been reached, which enables activation of molecular processes necessary to start (Jeffers and Shibles, 1969). Therefore, lower temperature generally decreases tree growth (Way and Oren, 2010). The response of growth to low air temperature was not simply decelerating the same trajectory of ontogeny achieved at optimal temperatures. Remarkably, temperature shifted the trajectory. When air temperature decreased from 25 to 12°C, orange tree was shorter with less foliage and more roots, as shown in Figure 8b. Moreover, the total biomass (Figure 13) of the 6-years-old orange tree decreased about 33.9% (from 6.43 to 4.25) showing a good agreement between simulation

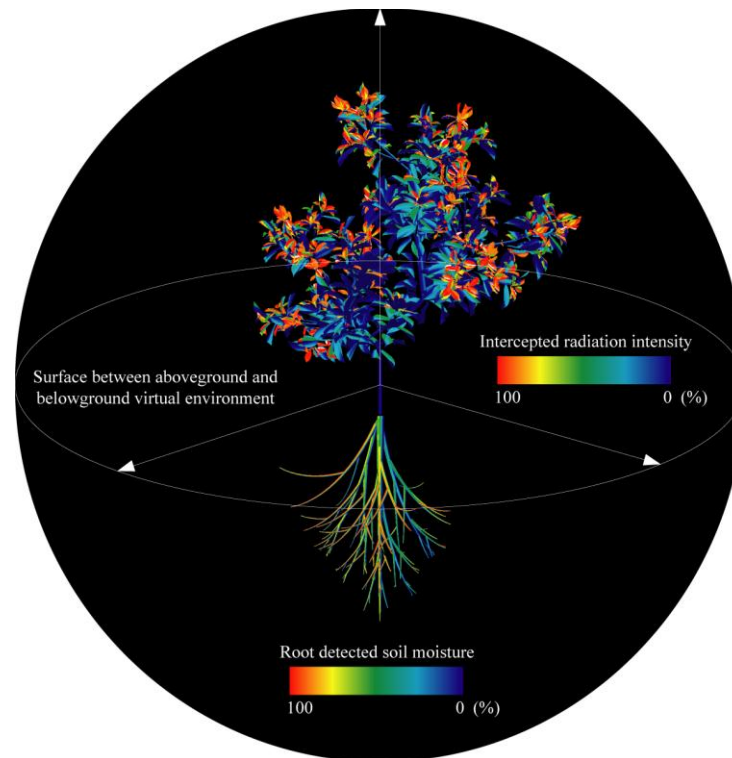


Figure 9. A snapshot of real time simulation of leaf intercepted radiation intensity and root detected soil moisture in aboveground and belowground of virtual environment. Due to direct and scatter radiation as well as crown distribution, the aboveground leaves illustrate their actual intercepted light intensity via being marked by different colors, and the same done.

and observation. The main reason to this decrease is that the lower temperature can dramatically decrease the fruit bearing percentage. Tree respiration responded less than photosynthesis to decreased temperature, because respiration acclimated while photosynthesis did not. Therefore respiration can not be the crucial determinant to tree biomass decrease.

Effects of water stress

Water deficit in soil results in stomatal closure and reduced transpiration rates, a decrease in the water potential of plant tissues, decrease in photosynthesis and growth inhibition. These physiological responses of trees are the underlying determinants make them undergo morphological changes. As shown in the simulation result (Figures 8d and 14), the morphological and physiological states of the simulated orange tree (which leaves were marked by yellow color) were significantly affected by water stress (30% FC). The primary visual effect of the water stress was a reduction in shoot growth. It exhibited a shorter branch height (decreased by 14.8% from 3.38 to 2.88 m), a smaller leaf area (decreased by 29.1% from

4.33 to 3.07 m²) than those of optimal one with full irrigation (100%FC), as shown in Table 3. The decrease of total biomass of root system was 58.9% (from 0.95 to 0.39 kg) due to water stress. When suffering water stress, measured reductions in total root biomass were indeed reproduced satisfactorily (Figure 14), although there is a slight deviation between the case of water stress ($R^2 = 0.7666$) and optimal condition ($R^2 = 0.8625$). Simulated biomass of orange tree was approximately 3.83 against measured 3.98 kg at the end of the 6 years development, that is to say very close to the actual measured values.

DISCUSSION

Due to the complex nature of tree branching pattern, it is very difficult to manually design growth rule for a specific woody plant (Barthélémy and Caraglio, 2007). Traditional plant structural models (Sievänen et al., 2000, 2004; Perttunen et al., 1996, 1998, 2001) are commonly confronted with this problem (Qu et al., 2009). Not to mention that all individual plants are distinct entities exhibiting behavior typical of all complex organisms (Trewaves, 2005), for example, preferential organ

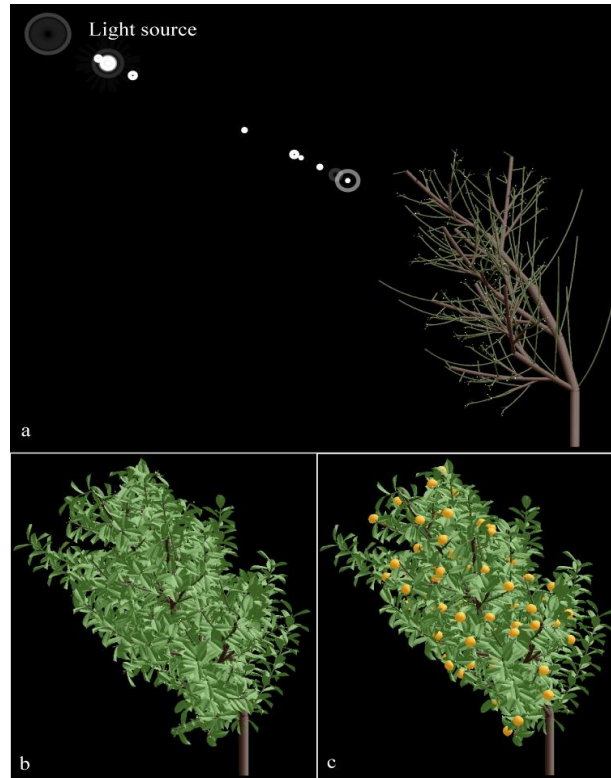


Figure 10. Simulated phototropism of orange tree with structure adaptation (a). Fully growing form with leaf cover and fruit production of the same orange tree were given in (b) and (c).

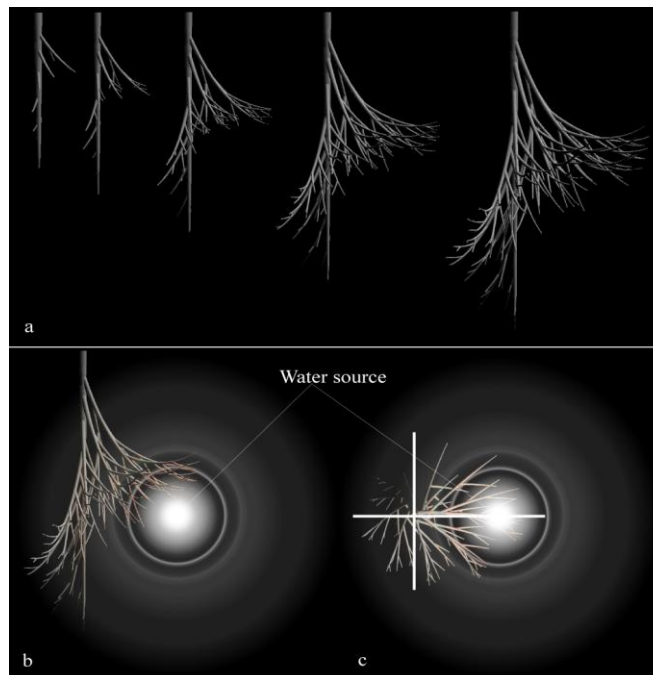


Figure 11. Simulated procedure of hydrotropism for root system of an orange tree (a). Panel (b) and (c) show the relative position between root and water source respectively in front and top view.

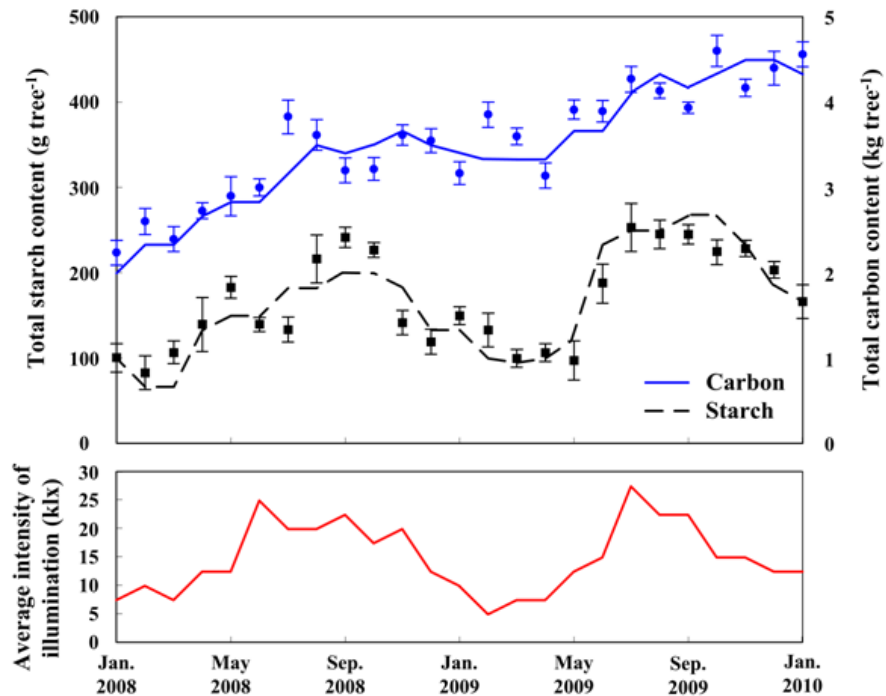


Figure 12. Simulation outputs of ORASIM: Effects of light intensity on total carbon content variation and reserve dynamics of orange tree from measurement (symbols) and simulation (lines). Weather data (red line) are average intensity of illumination (klx) measured at field site from Jan. 2008 to Jan. 2010. Vertical bars represent standard error of mean (n = 16).

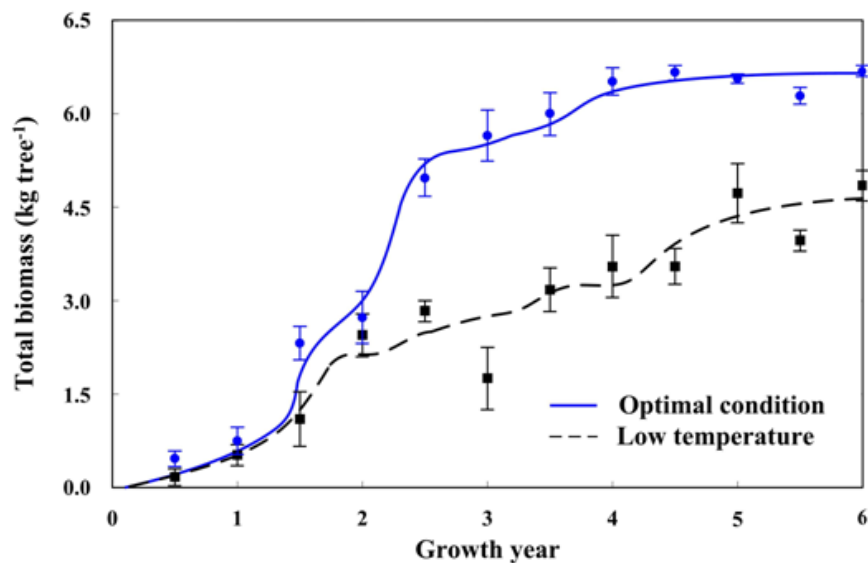


Figure 13. Simulation outputs of ORASIM: comparison of 6-years total biomass variations of orange trees simulated in optimal condition and in low air temperature from measurement (symbols) and simulation (lines). Vertical bars represent standard error of mean (n = 17).

placement of nutrients-foraging and light-stimulation, differential distribution of biomass as consequences of

environmental heterogeneity, etc. Although previous model (Colasanti and Hunt, 1997, 2001) can simulate

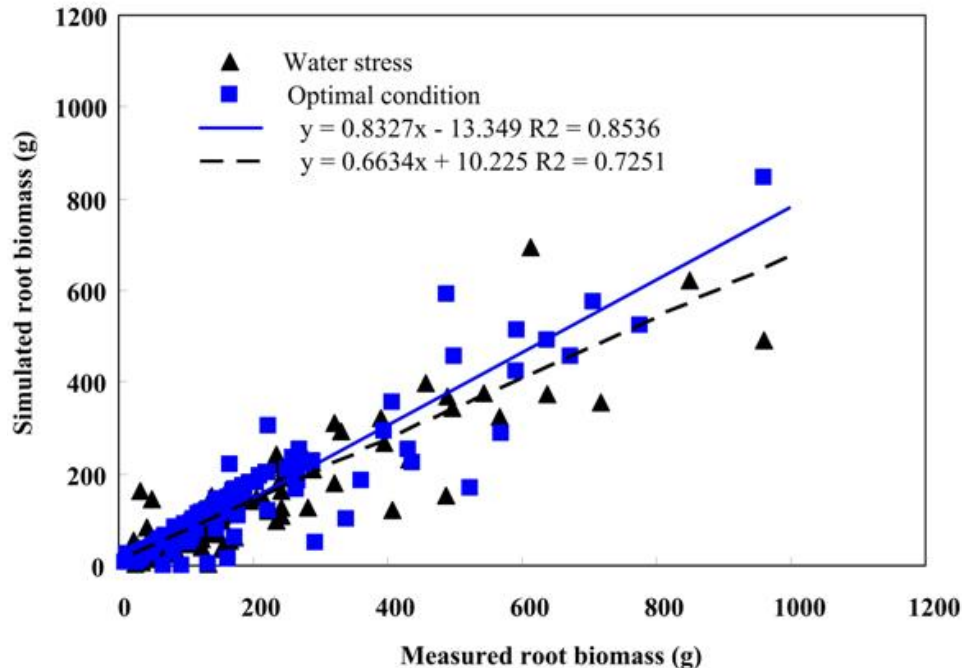


Figure 14. Simulation outputs of ORASIM: comparison between measured and simulated root biomass production for orange trees growing in optimal condition and suffering water stress.

plant adaptive behaviors in response to environmental constraints, it is still insufficient to induce typical growth patterns of real plants. The most important reason is that their cellular-automata-based model merely deals with external environment regulations. However, the internal determinant, gene controlled meristem states development was ignored, which is the endogenous mechanism that caused the branching pattern of a specific type of tree (Qu and Zhu, 2009).

Plant branching structure can be interpreted as the indirect transformation of different physiological states of the meristem, thus, connected entities may exhibit either similar or much contrasted characteristics. During the last decades, some statistical models (for example, Hidden semi-Markov chain, Hidden Markov tree, semi-Markov switching linear mixed model, etc.) have been employed by botanists and statisticians to discover and characterize homogeneous entity zones and transitions between them in different temporal scales within plant topological and geometrical data. These analyses and models lead to a clustering of the entities into classes sharing the similar statistical properties that help to find the tendency of the differentiation of meristem. One limitation of these stochastic methods must be mentioned is that one assume that the transitions of botanical entities conform to the first-order Markov dynamics, because the first order model is enough to reflect the statistical properties of plants and also is easy to be learned.

Trees are able to modify their foliage architecture in response to the incident angle of light source (Firn, 1994). Typically, phototropic response is dominated by

the blue region of the spectrum. This effect is mediated at least partially by phototropins (Briggs et al., 2001) which can drive the reorientation of leaves at early ontogenic stages of trees (Girardin, 1992; Maddonni et al., 2001). ORASIM models orange tree phototropism by producing new metamer with relative angles (the azimuth and inclination) respect to its parent. Once a bud of a metamer agent accumulated enough carbon and prepared to generate a new metamer, the azimuth and inclination angles related to its parent should be chosen according to which angles can make the new leaf get the maximum light (equation 35). This process was autonomously controlled by the reasoning cycle of the metamer agent.

In contrast with the branching rotation model employed in ORASIM, several simulation approaches (Chikushi and Hirota, 1998; Pagès 2000; Somporn et al., 2004) modeled the hydrotropism by root cap sensing rather than branching rotation. These models also used nutrient concentration as catalyst. The position of root apices will move to the appropriate nutrient concentration. The common advantage of these models and our approach used in ORASIM is that no rule for representing the root structure and root growth needed. Compared to ORASIM, most carbon-based plant growth models generally ignore or treat very briefly with the carbon storage/mobilization dynamics (Roux et al., 2001). This is because the current status of knowledge in this area makes it very difficult to represent storage/mobilization dynamics efficiently (Lacointe, 2000). Several models (Thomley, 1991; Wermelinger et al., 1991; Escobar-Gutierrez et al., 1998)

designed a specific reserve carbon pool separate from the current photosynthates for plant and made it simply to be a proportion of the total dry matter. However, this might not hold in the long term or on a wide range of disturbance, for example, the large amount of mobilization of starch in spring season. Consider this problem, more internal and external variables as well as, smart techniques (for example, intelligent modeling approaches employed in ORASIM) should be a good option to handle it.

Conclusion

Tree growth modeling and simulation so far has concentrated either on architectural aspects or on a functional characterization of processes. The simulation framework ORASIM presented in this work is based on autonomous metamer and root agents integrating physiological behaviors, and combines them with architectural explicitness being faithful to vivid real tree like branching pattern. In contrast with previous tree models and simulations, it allows to investigate how the overall structure, carbon dynamics and productivity of the fruit tree that develops over many years depends on the interplay of intelligent agents in terms of (a) physiological processes; (b) the response of morphological structure to the physiological status; and (c) inferences of environmental heterogeneity. The fundamental advantage of ORASIM is the capability to investigate, how model specifications of physiological features which are hard to measure (e.g., carbon transportation, allocation and redistribution) influence the resulting overall tree structure under specific environmental stimulations. One exciting aspect of ORASIM is that the orange tree simulated in ORASIM can be viewed as a complex adaptive system. The orange tree was modeled as complex organisms. Its growth and development exhibits behavior typical of all intelligent systems. In this way, the emergent structural and physiological phenomenon can be used to examine and hypotheses about the underlying functional specifications. Moreover, unlike conventional mechanistic models of complex or intelligent systems are usually highly time-consuming to build, difficult to parameterize and most unfriendly in use. Alternatively, a goal-seeking approach, the teleonomic model employed in ORASIM may provide a simple and easily applicable option which is of value for virtual plants.

ACKNOWLEDGEMENTS

We acknowledge the support of National Natural Science Foundation of China (61102145), the Research Project of Science and Technology of Chongqing Department of Education (KJ110520) and the Doctoral Start-Up Fund of Chongqing University of Posts and Telecommunications (A2010-19)).

REFERENCES

- Amthor JS (1984). The role of maintenance respiration in plant-growth, *Plant Cell Environ.*, 7: 561-569.
- Barthélémy D (2007). Caraglio Y, Plant architecture: A dynamic, multilevel and comprehensive approach to plant form, structure and ontogeny, *Ann. Bot.*, 99: 375-407.
- Botkin, DB, Janak JF, Wallis JR (1972). Some ecological consequences of a computer model of forest growth. *J. Ecol.*, 60: 849-872.
- Bradshaw AD (2006). Unravelling phenotypic plasticity – why should we bother? *New Phytol.*, 170: 644-648.
- Breckling B, Müller F, Reuter H, Hölker F, Fränze O (2005). Emergent properties in individual-based ecological models—introducing case studies in an ecosystem research context. *Ecol. Model.*, 186: 376-388.
- Briggs WR, Beck CF, Cashmore AR, Christied JM, Hughes J, Jarillo JA, Kagawa T, Kanegae H, Liscum E, Nagatani A (2001). The phototropin family of photoreceptors. *Plant Cell*, 13: 993-997.
- Chikushi J, Hirota O (1998) Simulation of root development based on the dielectric breakdown model. *Hydrological Sciences – J. Des. Sci. Hydrol.*, 43: 549-560.
- Colasanti RL, Hunt R (1997). Resource dynamics and plant growth: A self-assembling model for individuals, populations and communities. *Funct. Ecol.* 11: 133-145.
- Colasanti RL, Hunt R, Askew AP (2001). A self-assembling model of resource dynamics and plant growth incorporating plant functional types. *Funct. Ecol.*, 15: 676-687.
- Coleman M (2007). Spatial and temporal patterns of root distribution in developing stands of four woody crop species grown with drip irrigation and fertilization. *Plant Soil*, 299: 195-213.
- Cooper AJ (1973). Root temperature and plant growth, *Research Review No. 4*, Commonwealth Agricultural Bureaux, p. 73
- Deleuze C, Houllier F (1995). Prediction of stem profile of *Picea-Abies* using a process-based tree growth-model, *Tree Physiol.*, 15: 113-120.
- Dewar RC (1995). Interpretation of an empirical model for stomatal conductance in terms of guard cell function. *Plant, Cell Environ.*, 18: 365-372.
- Dingman SL (2002). "Chapter 6, Water in soils: infiltration and redistribution". *Physical Hydrology* (Second ed.). Upper Saddle River, New Jersey: Prentice-Hall, Inc.. p. 646. ISBN 0-13-099695-5.
- Drouet JL, Pagès LG (2003). A model of Growth, Architecture and carbon allocation during the vegetative phase of the whole maize plant: Model description and parameterization. *Ecol. Model.*, 165: 147-173
- Drouet JL, Pagès LGC (2007). A model of Growth, Architecture and Allocation for Carbon and Nitrogen dynamics within whole plants formalised at the organ level. *Ecol. Model.*, 206: 231-249.
- Eapen D, Barroso ML, Ponce G, Mari'a EC, Gladys IC (2005). Hydrotropism: root growth responses to water. *Trends Plant Sci.*, 10 44-50.
- Eschenbach C (2005). Emergent properties modelled with the functional structural tree growth model ALMIS: computer experiments on resource gain and use. *Ecol. Model.*, 186 470-488.
- Escobar-Gutierrez AJ, Daudet FA, Gaudillere JP, Maillard P, Frossard JS (1998). Modelling of allocation and balance of carbon in walnut (*Juglans regia* L.) seedlings during heterotrophy–autotrophy transition. *J. Theor. Biol.*, 194: 29-47.
- Filleur S, Walch-Liu P, Gan Y, Forde BG (2005). Nitrate and glutamate sensing by plant roots. *Biochem. Soc. Trans.*, 33: 283-286.
- Firn RD (1994). Phototropism. In RE Kendrick, GHM Kronenberg, eds, *Photomorphogenesis in Plants*. Kluwer Academic Publishers, Dordrecht, The Netherlands, 659-681.
- Fitter AH (2002). Characteristics and functions of root systems. In: Waisel, Y., Eshel, A., Kafkafi, U.P. (Eds.), *Plant Roots, the Hidden Half*. Marcel Dekker Inc., New York, pp. 15-32.
- Gao Q, Zhao P, Zeng X, Cai X (2002), Shen W, A model of stomatal conductance to quantify the relationship between leaf transpiration, microclimate and soil water stress. *Plant Cell Environ.*, 25: 1373-1381.
- Girardin P (1992). Leaf azimuth in maize canopies. *Eur. J. Agron.*, 1: 91-97.

- Hunt R, Colasanti RL (2007). Self-assembling plants and integration across ecological scales. *Ann. Bot.*, 100: 677-678.
- Coleman M (2007). Spatial and temporal patterns of root distribution in developing stands of four woody crop species grown with drip irrigation and fertilization. *Plant Soil*, 299: 195-213.
- Hallé, F, Oldeman RAA, Tomlinson PB (1978). *Tropical trees and forests: an architectural analysis*. Springer-Verlag, Berlin, p. 441.
- Genard M (2008). Carbon allocation in fruit trees: From theory to modelling. *Trees-Struct. Funct.*, 22: 269-282.
- Godin C, Costes E, Sinoquet H (1999). A Method for describing plant architecture which integrates topology and geometry. *Annu. Bot.*, 84: 343-357.
- Godin C (2000) Representing and encoding plant architecture: A review. *Ann. For. Sci.*, 57: 413-438.
- Goudriaan J (1977). *Crop micrometeorology. A simulation study*, Simulation monographs, Centre for Agricultural Publishing and Documentation, Wageningen,
- Host GE, Rauscher HM, Isebrands JG (1990). Michael DA. Validation of photosynthate production in ECOPHYS, an ecophysiological growth process model of Populus. *Tree Physiol.*, 7: 283-296.
- Jaeger M (1992). Reffye (de), Ph. Basic concepts of computer simulation of plant growth. *J. Biosci.*, 17: 275-291.
- Jourdan C, Rey H (1997). Modelling and simulation of the architecture and development of the oil-palm (*Elaeis guineensis* Jacq) root system.1. The model, *Plant Soil*, 190: 217-233.
- Katrin K, Dirk W, Hartmut SI (2008). Modelling leaf phototropism in a cucumber canopy. *Funct. Plant Biol.*, 35: 876-884.
- Kurth W (1994). Morphological models of plant growth: possibilities and ecological relevance. *Ecol. Model.*, 75/76: 299-308.
- Kurth W (2000). Towards universality of growth grammars: Models of Bell, Pagès, and Takenaka revisited. *Ann. For. Sci.*, 57: 543-554.
- Lacointe AK, Améglio T, Daudet FA, Cruiziat P, Archer P, Frossard JS (1993). Storage and mobilization of carbon reserves in walnut and its consequences on the water status during dormancy, *Acta Hortic.*, 311: 201-209.S
- Lacointe A (2000). Carbon allocation among tree organs: A review of basic processes and representations in functional-structural tree models. *Ann. For. Sci.*, 57: 521-533.
- Landsberg JJ (2003). Modelling forest ecosystems: state of the art, challenges, and future directions. *Can. J. For. Res.*, 33: 385-397.
- Landsberg, JJ, Waring RH (1997). A generalised model of forest productivity using simplified concepts of radiation-use efficiency, carbon balance and partitioning. *For. Ecol. Manage.*, 95: 209-228.
- Le Dizès S (1998). *Modélisation des relations structure-fonction du noyer; application à la taille*, Ph.D. Thesis, University of Orsay, France, p. 205.
- Le Roux X, Lacointe A, Escobar-Gutierrez A, Le Dizès S (2001). Carbon-based models of individual tree growth: A critical appraisal. *Ann. For. Sci.*, 58: 469-506.
- Li FL, Bao WK, Wu N (2009). Effects of water stress on growth, dry matter allocation and water-use efficiency of a leguminous species, *Sophora davidii*. *Agrofor. Syst.*, 77: 193-201.
- Lincoln Taiz EZ (2004). *Plant Physiology*, fourth ed., Wadsworth Publishing Co Inc.,
- Lynch J (1995). Root architecture and plant productivity. *Plant Physiol.*, 109: 7-13.
- Maddonni GA, Chelle M, Drouet J-L, Andrieu B (2001). Light interception of contrasting azimuth canopies under square and rectangular plant spatial distributions: simulations and crop measurements. *Field Crop Res.*, 70: 1-13.
- Mäkelä A, Hari P (1986). Stand growth model based on carbon uptake and allocation in individual trees. *Ecol. Model.*, 33: 205-229.
- Mäkelä A (1997). A carbon balance model of growth and self-pruning in trees based on structural relationships. *For. Sci.*, 43: 7-24.
- Marcelis LFM, Elings A, Dieleman JA (2002). in: L.F.M. Marcelis, G. VanStraten, C. Stanghellini, E. Heuvelink (Eds.), *Modelling dry matter production and partitioning in sweet pepper*, Third International Symposium on Models for Plant Growth, Environmental Control and Farm Management in Protected Cultivation, October 29–November, International Society Horticultural Science, Wageningen, Netherlands, pp. 121-128.
- Maillette L (1990). The Value of Meristem States, as Estimated by a Discrete-Time Markov Chain. *Oikos*, 59: 235-240.
- Martin GL, Ek AR (1984). A comparison of competition measures and growth models for predicting plantation red pine timber and height growth. *For. Sci.*, 30: 731-743.
- McMurtrie RE, Landsberg JJ (1992) Using a simulation model to evaluate the effects of water and nutrients on growth and carbon partitioning of Pinus radiata. *For. Ecol. Manage.*, 52: 243-260.
- Minchin PEH, Thorpe MR, Farrar JF (1993). A simple mechanistic model of phloem transport which explains sink priority. *J. Exp. Bot.*, 44: 947-955.
- Mulia R, Dupraz C (2006). Unusual Fine Root Distributions of Two Deciduous Tree Species in Southern France: What Consequences for Modelling of Tree Root Dynamics? *Plant and Soil*, 281: 71-85.
- Nygren P, Kiema P, Rebottaro S (1996). Canopy development, CO2 exchange and carbon balance of a modelled agroforestry tree. *Tree Physiol.*, 16: 733-745.
- Pages L (1999). Root system architecture: from its representation to the study of its elaboration, *Agronomie*, 19: 295-304.
- Pagès L (2000). How to include organ interactions in models of the root system architecture? The concept of endogenous environment. *Ann. For. Sci.*, 57: 535-541.
- Perttunen J, Sievänen R, Nikinmaa E, Salminen H, Saarenmaa H, Väkevä J (1996). LIGNUM: A tree model based on simple structural units. *Ann. Bot.*, 77: 87-98.
- Perttunen J, Sievänen R, Nikinmaa E (1998). LIGNUM: A model combining the structure and the functioning of trees. *Ecol. Model.*, 108: 189-198.
- Perttunen J, Nikinmaa E, Lechowicz MJ, Sievänen R, Messier C (2001). Application of the functional-structural tree model LIGNUM to sugar maple saplings (*Acer saccharum* Marsh) growing in forest gaps. *Ann. Bot.*, 88: 471-481.
- Prentice IC, Sykes MT, Cramer W (1993). A simulation model for the transient effects of climate change on forest landscapes. *Ecol. Model.*, 65: 51-70.
- Prusinkiewicz, P, Hanan J (1989). Lindenmayer systems fractals and plants. 79 in *Lecture notes in biomathematics*. Springer-Verlag, Berlin.
- Prusinkiewicz, P, Hanan J (1992). L-systems: From formalism to programming languages. In: G. Tozengerg, A. Salomaa (eds.): *Lindenmayer Systems*. Springer, Berlin, pp. 193-211.
- Pruzinkiewicz, P (2001). The use of positional information in the modeling of plants. In: *ACM SIGGRAPH 2001*, 12-17 August, Los Angeles, CA, USA, pp. 289-300.
- Prusinkiewicz, P (2004). Modeling plant growth and development. *Current Opinion in Plant Biology*. 7: 79-83.
- Prusinkiewicz P, Karwowski R, Me'ch R (2004). The L-system-based plant-modeling environment L-studion 4.0, in: *Proceedings of the Fourth International Workshop on Functional–Structural Plant Models*, 07–11 June, Montpellier, France, pp. 403-405.
- Qu HC, Zhu QS, Deng QQ, Zeng LQ, Ge L (2007) Modelling and constructing of intelligent physiological engine merging artificial life for virtual plants. *J. Comput. Theor. Nanos.* 4: 1405-1411.
- Qu HC, Zhu QS (2009). Automatic Approaches to Plant Meristem States Revelation and Branching Pattern Extraction: A Review. In *Pattern Recognition*, Book edited by: Peng-Yeng Yin, ISBN: 978-953-307-014-8, Publisher: INTECH, Publishing date: October.
- Qu HC, Zhu QS, Guo MW, Lu ZH (2009). An intelligent learning approach to L-grammar extraction from image sequences of real plants, *Int. J. Artif. Intell. Tools*, 6: 905-927.
- QuH.C, Zhu QS, Guo MW, Lu ZH (2010). Simulation of carbon-based model for virtual plants as complex adaptive system. *Simul. Model. Pract. Theor.*, 18: 677-695
- Railsback SF (2001). Concepts from complex adaptive systems as a framework for individual-based modelling, *Ecol. Model.*, 139: 47-62.
- Rauscher HM, Isebrands JG, Host GE, Dickson RE, Dickmann DI, Crow TR, Michael DA (1990). ECOPHYS: an ecophysiological growth process model for juvenile poplar. *Tree Physiol.*, 7: 255-281.
- De Reffye PH, Houllier F, Blaise F, Barthélémy D, Dauzat J, Auclair D (1995). A model simulating above- and below-ground tree architecture with agroforestry applications. *Agroforestry Systems*. 30: 175–197
- Reffye PH, Fourcaud T, Blaise FA (1997). Functional model of tree

- growth and tree architecture. *Silva Fennica*, 31: 297-311
- Reffye P, Hu, BG, Habib R, Hu BG, Jaeger M (2003). Relevant qualitative and quantitative choices for building an efficient dynamic plant growth model: Greenlab case, in: *Plant Growth Modeling and Applications Proceedings – PMA03, International Symposium on Plant Growth Modeling, Simulation, Visualization and their Applications*, October 13–16, 2003, Tsinghua University Press, Springer, Beijing, China, pp. 87-107.
- Richardson EA, Seeley SD, Walker DR (1974). A model for estimating the completion of rest for Redhaven and Elberta peach trees. *Hortscience*, 9(4): 331-332.
- Riedacker A (1976). Rythmes de croissance et de régénération des racines des végétaux ligneux. *Ann. Sci. For.*, 33: 109-138.
- Robinson AP, Ek AR (2000). The consequences of hierarchy for modeling in forest ecosystems. *Can. J. For. Res.*, 30: 1837-1846.
- Room PM, Maillette L, Hanan JS (1994). Module and metamer dynamics and virtual plants, in: *Adv. Ecol. Res.*, 25: 105-157.
- Shinozaki K, Yoda K, Hozumi K, Kira T (1964). A quantitative analysis of plant form - the pipe model theory. I. Basic analyses. *Jpn. J. Ecol.*, 14: 97-105.
- Sievänen R, Nikinmaa E, Nygren P, Ozier-Lafontaine H, Perttunen J, Hakula H (2000). Components of functional-structural tree models. *Ann. For. Sci.*, 57: 399-412
- Sievänen R, Perttunen J, Nikinmaa E, Berninger F, Nygren P (2004). Modelling tree development with transport/conversion approach in branched architecture. 4th International Workshop on Functional-Structural Plant Models, Montpellier. 7-11 June.
- Smit AL, Bengough AG, Engels C, van Noordwijk M, Pellerin S, van de Geijn SC (2000). *Root Methods: A Handbook*, Springer-Verlag Berlin Heidelberg New York.
- Somma F, Clausnitzer V, Hopmans JW (1997). An algorithm for three-dimensional, simultaneous modeling of root growth, transient soil water flow, and solute transport and uptake, V. 2.1, Paper no. 100034, Dept. of Land, Air, and Water Resources, U. of Calif., Davis,
- Somma F, Hopmans JW, Clausnitzer V (1998). Transient three-dimensional modeling of soil water and solute transport with simultaneous root growth, root water and nutrient uptake. *Plant and Soil*, 202: 281-293.
- Somporn CA, Willi J, Hans GB, Suchada S (2004). Modeling, simulation and visualization of plant root growth and diffusion processes in soil volume. in: *Proceedings of the Fourth International Workshop on Functional-Structural Plant Models*, C. Godin et al. (eds.), 07–11 June, Montpellier, France, pp. 289-293.
- Sprugel D, Benecke U (1991). Woody-tissue respiration and photosynthesis, in: J. Lassoie, T. Hinckley (Eds.), *Technics and Approaches in Forest Tree Ecophysiology*, CRC Press, Boca Raton, FL, USA, 1991.
- Sterck FJ, Schieving F, Lemmens A, Pons TL (2005). Performance of trees in forest canopies: explorations with a bottom-up functional-structural plant growth model. *New Phytol.*, 166: 827-843.
- Sterck FJ, Schieving F (2007). 3-D growth patterns of trees: effects of carbon economy, meristem activity, and selection. *Ecol. Monogr.*, 77: 405-420.
- Takenaka A (1994). Effects of leaf blade narrowness and petiole length on the light capture efficiency of a shoot. *Ecol. Res.*, 9: 109-114.
- Theseira GW, Host GE, Isebrands JG, Whisler FD (2003). SOILPSI: A potential-driven three-dimensional soil water redistribution model—description and comparative evaluation. *Environ. Model. Softw.*, 18: 13-23.
- Thompson MV, Holbrook NM (2003). Application of a single-solute non-steady-state phloem model to the study of long-distance assimilate transport. *J. Theor. Biol.*, 220: 419-455.
- Thornley JHM (1991). A transport-resistance model of forest growth and partitioning. *Ann. Bot.*, 68: 211-226.
- Trewavas A (2005). Plant intelligence, *Naturwissenschaften*, 92: 401-413.
- van den Berg C, Willemsen V, Hage W, Weisbeek P, Scheres B (1995). Cell fate in the Arabidopsis root meristem determined by directional signalling, *Nature*, 378: 62-65.
- van den Berg M, Driessen PM (2002). Water uptake in crop growth models for land use systems analysis: I. A van den Berg M, review of approaches and their pedigrees. *Agric. Ecosyst. Environ.*, 92: 21-36.
- Driessen PM, Rabbinge R (2002). Water uptake in crop growth models for land use systems analysis: II. Comparison of three simple approaches. *Ecol. Model.*, 148: 233-250.
- Vos J, Evers JB, Buck-Sorlin GH (2009). Functional-structural plant modelling: a new versatile tool in crop science. *Journal of Experimental Botany*, doi:10.1093/jxb/erp345.
- Vrugt JA, Hopmans JW, Simunek J (2001). Calibration of a Two-Dimensional Root Water Uptake Model. *Soil Sci. Soc. Am. J.*, 65: 1027-1037
- Walsh JWT (1961). *The science of daylight*, Mac Donald, London, p. 291.
- Wang E, Smith C (2004). Modelling the growth and water uptake function of plant root systems: a review. *Aust. J. Agric. Res.*, 55: 501-523.
- Wang H, Yamauchi A (2006). Growth and function of roots under abiotic stress in soil. In: Huang, B. (Ed.), *Plant-Environment Interactions*, 3rd ed. CRC Press, New York, pp. 271-320.
- Wang YP, Jarvis PG (1990) Description and validation of an array model - MAESTRO. *Agric. For. Meteorol.*, 51: 257-280.
- Wardlaw IF (1990). Tansley Review No. 27 – the Control of Carbon Partitioning in Plants, *New Phytol.*, 116: 341-381.
- Way DA, Oren R (2010). Differential responses to changes in growth temperature between trees from different functional groups and biomes: a review and synthesis of data. *Tree Physiol.*, 30: 669-688.
- Weinstein DA, Yanai RD (1994) Integrating the effects of simultaneous multiple stresses on plants using the simulation model TREGRO. *J. Environ. Qual.*, 23: 418-428.
- Weiss A, Norman JM (1985). Partitioning solar radiation into direct and diffuse, visible and near-infrared components. *Agric. For. Meteorol.*, 34: 205-213.
- Wermelinger B, Baumgartner J, Gutierrez AP (1991). A demographic-model of assimilation and allocation of carbon and nitrogen in grapevines. *Ecol. Model.*, 53: 1-26.
- Williams M (1996). A three-dimensional model of forest development and competition. *Ecol. Model.*, 89: 73-98.
- Wright CJ (1989). *Interactions between vegetative and reproductive growth*, Butterworths, London, UK, 1989.
- Yan HP, Kang MZ, Reffye P (2004). De, Dingkuhn M., A dynamic, architectural plant model simulating resource-dependent growth. *Ann. Bot.*, 93: 591-602.
- Yang Z, David J (2005). Midmore. Modelling plant resource allocation and growth partitioning in response to environmental heterogeneity. *Ecol. Model.*, 181: 59-77.
- Yin X, Van Laar HH (2005). Crop systems dynamics: an ecophysiological simulation model for genotype-by-environment interactions. Wageningen Academic, Wageningen.